

Paper Type: Original Article

## Numerical Investigation of the Effect of Discrete Ribs on Flow Field and Heat Transfer in a Rectangular Channel

Hamed Mohaddes Deylami\* 

Faculty of Mechanical Engineering, University of Guilan, Iran; hmohaddesd@gmail.com.

### Citation:

Received: 9 January 2025

Revised: 5 March 2025

Accepted: 17 May 2025

Mohaddes Deylami, H. (2025). Numerical investigation of the effect of discrete ribs on the flow field and heat transfer in a rectangular channel. *Mechanical Technology and Engineering Insights*, 2(3), 151-161.


### Abstract


Enhancement of convective heat transfer in internal cooling channels is of great importance in the design of compact heat exchangers, turbine blade cooling passages, and electronic thermal management systems. In the present study, a comprehensive numerical investigation is conducted to analyze the effects of discrete ribs on the flow field and heat transfer characteristics in a two-dimensional rectangular channel. Three different rib geometries, namely triangular, rectangular, and circular ribs, are examined under turbulent forced convection conditions using air as the working fluid. The Reynolds-averaged Navier–Stokes equations coupled with the energy equation are solved using the finite element method implemented in COMputer SOLution (COMSOL) multiphysics. Turbulence effects are modeled using the  $k-\omega$  SST model to accurately capture flow separation, recirculation zones, and near-wall behavior induced by the ribs. A constant heat flux is applied to the ribbed wall, while the remaining walls are assumed adiabatic. A detailed grid independence study and validation against classical Nusselt number correlations are performed to ensure numerical accuracy. The effects of rib number, rib height, base length, and rib shape on velocity distribution, pressure loss, and Nusselt number are systematically investigated. The results demonstrate that discrete ribs significantly disturb the boundary layer, generate strong vortical structures, and enhance convective heat transfer compared to smooth channels. Increasing the number of ribs intensifies turbulence and heat transfer but also increases pressure losses. Rib geometry is shown to play a critical role: rectangular ribs provide the highest Nusselt number enhancement due to stronger, more persistent vortices. In contrast, shorter ribs reduce pressure penalties with moderate heat transfer improvement. The findings provide valuable insights into the optimal geometric design of ribbed channels for high-performance thermal systems.


**Keywords:** Convective heat transfer, Internal cooling channel, Discrete ribs, Turbulent flow, Heat transfer enhancement, Pressure drop, Numerical simulation, Vortex formation, Thermal performance, Channel geometry optimization.

## 1 | Introduction

Enhancing heat transfer in internal flows is a critical aspect in the design of high-performance heat exchangers, cooling channels, and energy conversion systems. Conventional smooth channels often exhibit

 Corresponding Author: hmohaddesd@gmail.com

 <https://doi.org/10.48313/mtei.v2i3.46>

 Licensee System Analytics. This article is an open access article distributed under the terms and conditions of the Creative Commons Attribution (CC BY) license (<http://creativecommons.org/licenses/by/4.0>).

limited heat transfer due to the development of laminar boundary layers and insufficient fluid mixing, particularly at moderate Reynolds numbers. To overcome these limitations, a variety of surface modifications and turbulence-promoting devices have been proposed, including ribs, dimples, protrusions, and vortex generators. Among these, discrete ribs have received considerable attention because of their ability to locally disrupt the boundary layer, generate secondary flows and vortices, and enhance convective heat transfer without excessively increasing pressure drop.

Liu and Wang [1] proposed a semi-attached rib design in 2011, in which the ribs were perforated at the corners to allow partial fluid passage. Numerical simulations using Fluent 6.3 over  $Re = 10^4$ – $2.5 \times 10^4$  demonstrated that semi-attached ribs could substantially improve local heat transfer and flow performance. Notably, semi-attached ribs with a  $45^\circ$  attack angle outperformed fully attached and detached ribs in overall thermal efficiency while eliminating low-heat-transfer regions.

Experimental studies by Tanda [2] in the same year investigated forced-convection heat transfer in rectangular channels with  $45^\circ$ -inclined rib turbulators. The effects of rib spacing and rib pitch-to-height ratios on thermal performance were systematically examined using Liquid Crystal Thermography (LCT), showing that optimal configurations can significantly enhance heat transfer for both single- and double-rib wall channels.

Chang et al. [3] introduced a novel Heat Transfer Enhancement (HTE) technique using deep V-shaped ribs. They experimentally investigated the heat transfer performance and pressure drop in a rectangular channel with these surfaces for both forward and backward flows over a Reynolds number range of 1,000–30,000. The HTE ratio, compared with smooth-wall conditions, showed significant improvement, particularly in laminar flow, with values ranging from 9.5 to 13.6 for forward flow. Moreover, the reduction in HTE with increasing Reynolds number in turbulent flow, which is a common limitation for many HTE devices, was mitigated by the combined HTE surfaces. Empirical correlations were also developed to support design applications.

Yemnisi et al. [4] performed an experimental analysis of airflow over successive rectangular ribs with varying heights and spacings. Their findings indicated that increased rib height enhanced turbulence, flow separation, and reattachment, leading to higher heat transfer rates than in smooth channels, with enhancements up to 113% in laminar flow and 50% in turbulent flow at the highest rib heights.

The numerical study by Yungseri et al. [5] on inclined discrete ribs demonstrated that rib attack angles significantly influenced turbulent flow behavior and heat transfer rates. At high Reynolds numbers, attack angles of  $60^\circ$  and  $120^\circ$  provided the highest thermal performance, while at low Reynolds numbers, the effect of rib inclination was minimal.

Shen et al. [6] numerically studied U-shaped channels with discrete ribs, showing increased Nusselt numbers and friction factors. The combined presence of protrusions and dimples was found to optimize heat transfer performance while minimally impacting pressure drop. Similarly, Parsaeimehr et al. [7] investigated turbulent nanofluid (water/ $Al_2O_3$ ) flow in rectangular channels with inclined ribs. Their results revealed that the rib attack angle, Reynolds number, and nanoparticle volume fraction all played key roles in enhancing convective heat transfer, with maximum enhancement occurring at a  $60^\circ$  attack angle.

Further studies in 2018 by Wang et al. [8] and Srinivasan et al. [9] emphasized the effects of rib geometry, spacing, and arrangement on both heat transfer and friction loss in rectangular channels. These studies collectively confirmed that discrete ribs can significantly improve thermal performance across a wide range of operating conditions.

Recent investigations by Liu et al. [10] and Shen et al. [6] focused on perforated and slotted ribs, highlighting the benefits of secondary flows induced by holes and slots in improving heat transfer efficiency while maintaining acceptable pressure drops. Experimental and numerical analyses demonstrated that perforated ribs can reduce recirculation zones behind ribs and provide more uniform heat transfer distributions, making them particularly promising for internal cooling applications such as turbine blade channels and high-performance electronics cooling.

Finally, Sivakumar et al. [11] examined rectangular divergent channels with square ribs and varying rib heights. They observed that moderate rib heights can significantly increase heat transfer while causing only minor increases in pressure drop, underscoring the potential for geometric optimization in practical applications.

Despite extensive studies on ribbed channels, several gaps remain. Most prior research focused on fully attached, detached, or semi-attached ribs under steady-state turbulent flows. In contrast, systematic investigations of the effects of discrete rib geometry, spacing, and orientation in conjunction with emerging fluids, such as nanofluids, remain limited. Moreover, the combined effects of rib inclination, perforation, and high-Reynolds-number turbulent flows on local and overall thermal performance are not yet fully understood. Addressing these gaps is crucial for designing advanced heat transfer surfaces in energy-intensive engineering applications.

In this study, a comprehensive numerical investigation is conducted to examine the effects of discrete ribs on flow structure and heat transfer in a rectangular channel. The influence of rib height, spacing, attack angle, and arrangement is systematically analyzed under both laminar and turbulent flow conditions. The outcomes aim to provide insights for the optimal design of ribbed surfaces in high-performance cooling and heat transfer systems.

## 2 | Problem Definition

This study focuses on turbulent convective heat transfer and flow behavior within a rectangular cavity with ribbed surfaces. The cavity is considered a simplified model of internal cooling passages commonly used in heat exchangers, turbine blade channels, and electronic cooling systems. The working fluid is air, entering the cavity at a uniform inlet velocity  $U_0$  and temperature  $T_0$ .

Three rib geometries are investigated: triangular, square, and circular ribs. The ribs are mounted on one of the cavity walls to disturb the boundary layer and promote secondary flows, thereby enhancing convective heat transfer. The number of ribs ( $N$ ) is also varied to examine its effect on both local and overall heat transfer rates.

The thermal boundary condition is a uniform heat flux applied to the ribbed wall, representing a constant heat source. The remaining walls are assumed adiabatic unless otherwise specified. The inlet is treated as a uniform-velocity, uniform-temperature boundary, and the outlet is assumed to be a pressure outlet, allowing fully developed flow.

The computational domain and rib configurations are schematically shown in *Figs. 1-3*. *Fig. 1* illustrates the rectangular cavity with triangular ribs, *Fig. 2* shows the cavity with square ribs, and *Fig. 3* depicts the cavity with circular ribs. These schematics highlight the geometric parameters, including rib height, width, and spacing, which are systematically varied to analyze their impact on the flow and heat transfer performance.

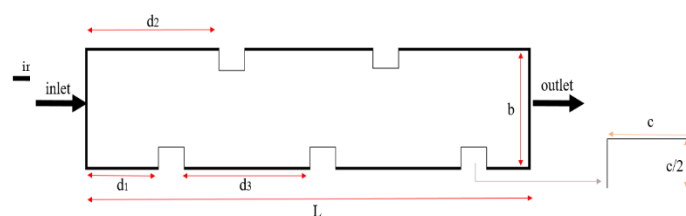


**Fig. 1.** Schematic of the rectangular cavity with triangular ribs.

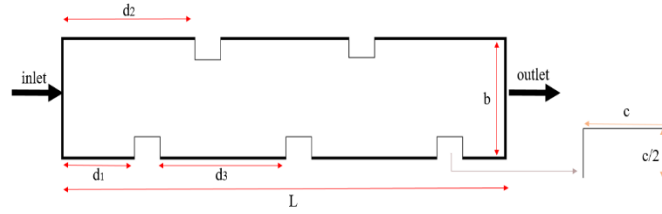


Fig. 2. Schematic of the rectangular cavity with square ribs.

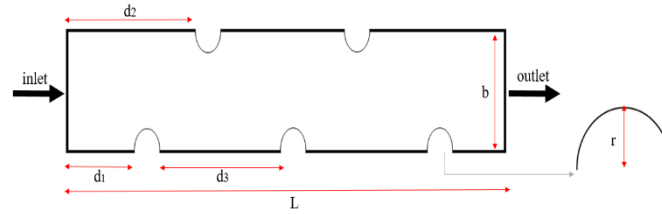


Fig. 3. Schematic of the rectangular cavity with circular ribs.

The geometric and operating parameters illustrated in *Figs 1-3* are summarized in *Table 1*. These parameters define the physical dimensions of the computational domain as well as the inlet flow and thermal boundary conditions employed in the present simulations. All parameters are kept constant unless otherwise stated to isolate the effects of rib geometry, rib spacing, and rib number on the flow field and heat transfer characteristics.

Table 1. Geometrical and operating parameters of the computational domain.

Description	Value	Parameter
Channel length	5 m	(L)
Channel height	0.5 m	(b)
Inlet temperature	283 K	( $T_0$ )
Inlet velocity	0.5 m/s	( $U_0$ )
Wall heat flux	10 W/m <sup>2</sup>	( $q_{-w}$ )
Mesh refinement coefficient	0.1	Mesh-coeff

## 3 | Governing Equations and Numerical Method

### 3.1 | Governing Equations

The turbulent forced-convection heat transfer of air flowing through a rectangular channel with discrete ribs is numerically investigated using a finite-element approach. The flow is assumed to be two-dimensional, steady-state, incompressible, and Newtonian. The effects of viscous dissipation and radiation are neglected, while the thermo-physical properties of air are assumed constant. The governing equations consist of the Reynolds-averaged continuity, momentum, and energy equations, expressed as follows:

$$\rho(\mathbf{u} \cdot \nabla)\mathbf{u} = \nabla \cdot [-p\mathbf{I} + \boldsymbol{\kappa}] + \mathbf{F}, \quad (1)$$

$$\rho \nabla \cdot \mathbf{u} = 0, \quad (2)$$

$$\boldsymbol{\kappa} = (\mu + \mu_T)(\nabla\mathbf{u} + (\nabla\mathbf{u})^T), \quad (3)$$

$$\rho(\mathbf{u} \cdot \nabla)k = \nabla \cdot \left[ \left( \mu + \frac{\mu_T}{\sigma_k} \right) \nabla k \right] + P_k - \rho\epsilon, \quad (4)$$

$$\rho(\mathbf{u} \cdot \nabla)\epsilon = \nabla \cdot \left[ \left( \mu + \frac{\mu_T}{\sigma_k} \right) \nabla \epsilon \right] + C_{\epsilon 1} \frac{\epsilon}{k} P_k - C_{\epsilon 2} \rho \frac{\epsilon^2}{k}, \quad \epsilon = \epsilon_p, \quad (5)$$

$$d_z \rho c_p \mathbf{u} \cdot \nabla T + \nabla \cdot \mathbf{q} = d_z Q + q_0 + d_z Q_p + d_z Q_{vd}, \quad (6)$$

$$\mathbf{q} = -d_z k \nabla T. \quad (7)$$

### 3.2 | Boundary Conditions

The applied boundary conditions are summarized as follows:

- I. Inlet: uniform velocity  $U_0$  and uniform temperature  $T_0$
- II. Outlet: pressure outlet with zero gauge pressure and fully developed flow assumption
- III. Ribbed wall: constant heat flux condition
- IV. Other walls: adiabatic condition

### 3.3 | Turbulence Modeling

To accurately capture flow separation, recirculation zones, and the enhanced mixing induced by discrete ribs, a Reynolds-Averaged Navier–Stokes (RANS) turbulence model is employed. Based on previous COMputer SOLution (COMSOL) investigations of ribbed channels, the  $k$ – $\omega$  SST turbulence model is selected for its superior performance in near-wall regions and its ability to accurately predict adverse pressure-gradient flows and separation.

The transport equations for turbulent kinetic energy  $k$  and specific dissipation rate  $\omega$  are solved simultaneously with the mean flow equations. The SST formulation blends the  $k$ – $\omega$  model near the wall with the  $k$ – $\epsilon$  model in the core flow, ensuring numerical stability and physical accuracy.

### 3.4 | Numerical Implementation in COMputer SOLution Multiphysics

The numerical simulations are carried out using COMSOL Multiphysics, which employs the finite element method (FEM) to discretize the governing equations. The modeling procedure follows a standard COMSOL workflow commonly reported in ISI-indexed CFD studies:

- I. The Model Wizard is used to define the problem.
- II. A 2D domain is selected because spanwise effects are negligible.
- III. The Turbulent Flow ( $k$ – $\omega$  SST) and Heat Transfer in Fluids physics interfaces are selected and fully coupled.
- IV. A Stationary study is employed to obtain steady-state solutions.

Air is selected from the COMSOL material library, and temperature-independent properties are used.

### 3.5 | Mesh Generation and Grid Independence

The computational domain is discretized using unstructured triangular elements, with boundary-layer refinement near walls and rib surfaces to accurately resolve velocity and thermal gradients. A mesh refinement coefficient of 0.1 is adopted.

## 4 | Result and discussion

A grid independence study is performed by refining the computational Mesh using the Mesh Coeff parameter. The average heat transfer coefficient is monitored as the primary convergence indicator.

As shown in *Table 2*, mesh refinement beyond Mesh Coeff = 0.1 results in variations of less than 1% in the predicted heat transfer coefficient. Therefore, this mesh resolution is adopted for all simulations.

**Table 2. Grid independence study**

Mesh Coeff	Number of elements	$h_{avg}$ (W/m <sup>2</sup> ·K)	Deviation (%)
0.30	18,420	12.86	–
0.20	31,750	13.21	2.72
0.15	46,980	13.38	1.29
0.10	68,540	13.44	0.45
0.08	92,610	13.46	0.15

The numerical model is validated using the classical benchmark of turbulent air flow over a smooth flat plate. The predicted heat transfer coefficient is compared with well-established Nusselt number correlations for turbulent forced convection. The reference correlations are adopted from Bejan and Kraus [12] and Lienhard [13], which are widely used in high-impact heat transfer studies. The numerical results show very good agreement with the correlation-based predictions, confirming the accuracy of the present numerical framework.

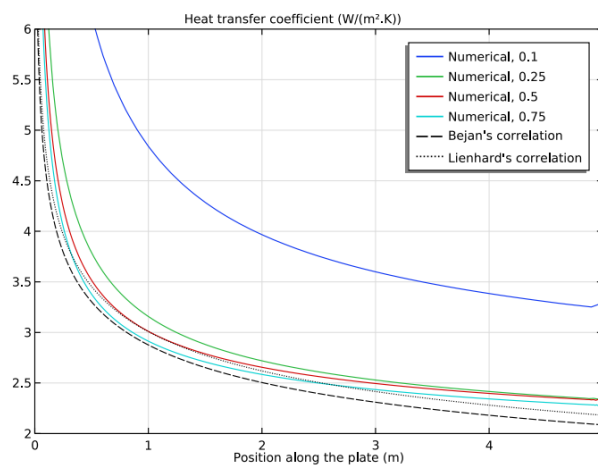


**Fig. 4. Comparison of the numerical heat transfer coefficient with Nusselt number correlation.**

The simulations were performed for a rectangular channel of length  $L = 1$  m and height  $b = 0.25$  m, with air entering at a temperature of  $T_0 = 293$  K and a velocity of  $U_0 = 0.1$  m/s under turbulent conditions. Eight different configurations were considered, varying the rib shape, size, and spacing. The geometrical parameters for each case are summarized in *Table 4*.

**Table 4. Geometrical parameters for different rib configurations.**

Case	Rib Shape	Number of Ribs	Rib Base [m]	Rib Height [m]	Rib Spacing [m]
1	Triangular	5	0.05	0.05	3
2	Triangular	9	0.05	0.05	1
3	Triangular	9	0.05	0.1	1
4	Triangular	9	0.05	0.025	1
5	Triangular	9	0.15	0.025	1
6	Rectangular	9	0.15	0.025	1
7	Rectangular	9	0.05	0.025	1
8	Rectangular	9	0.05	0.05	1

### 4.1 | Velocity Distribution

The velocity distribution along the channel is shown in *Fig. 5*, which shows that the flow interacts strongly with the ribs, inducing vortices and enhancing turbulence.

In Case 1 (5 triangular ribs), the velocity above the rib reaches approximately 0.2 m/s, while in the recirculation region behind the rib, the velocity drops close to zero. The vortices gradually decay until the flow reaches the next rib, where turbulence is regenerated.

In Case 2, increasing the number of ribs to 9 generates additional vortices, which prevent the flow from fully decelerating between ribs. Consequently, overall turbulence is higher.

In Cases 3 and 4, changing the rib height alters the vortex intensity. A taller rib in Case 3 (0.1 m) generates slightly weaker turbulence compared to Case 2, while a shorter rib in Case 4 (0.025 m) produces smaller disturbances, resulting in a more uniform velocity distribution.

For Cases 5–8 with rectangular ribs, the flow patterns and turbulence intensity depend on the rib dimensions. Maximum local velocity peaks and vortex activity are observed in Case 8.

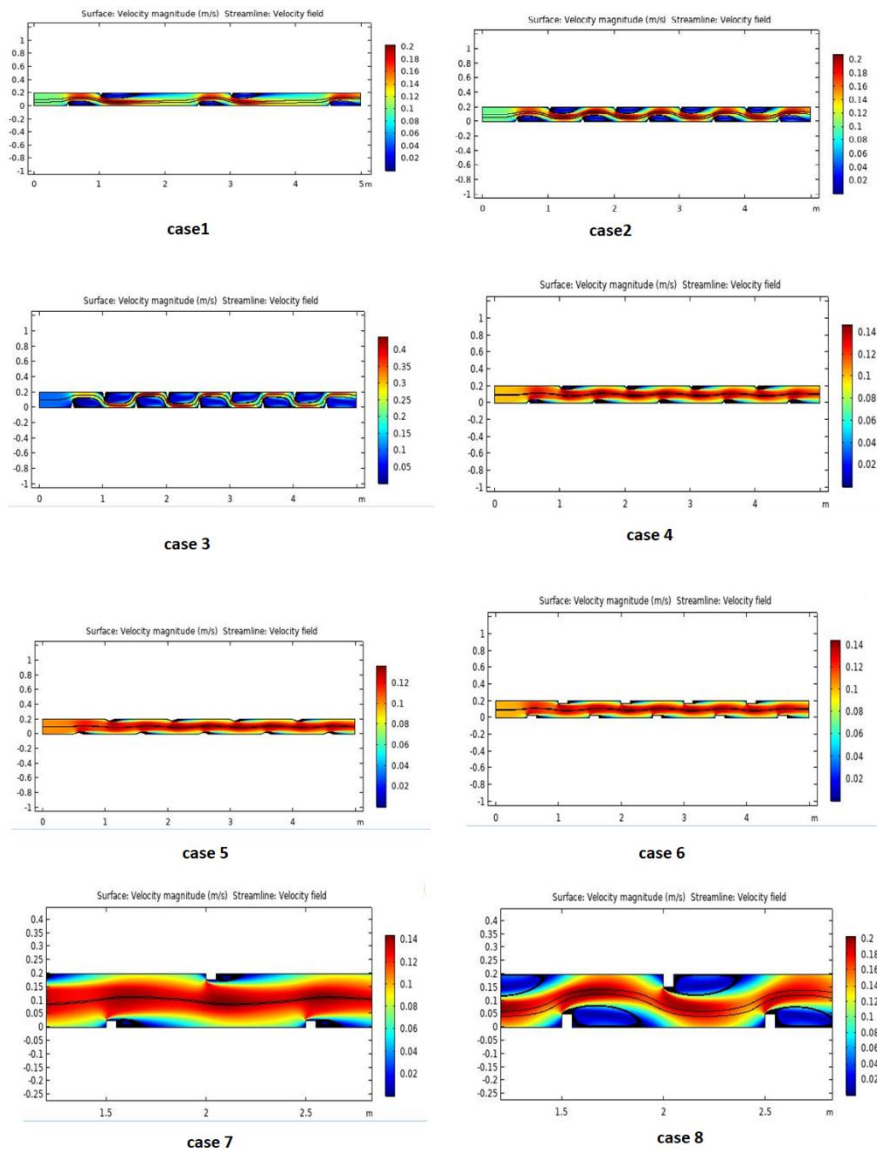


Fig. 5. The velocity distribution along the channel in all cases.

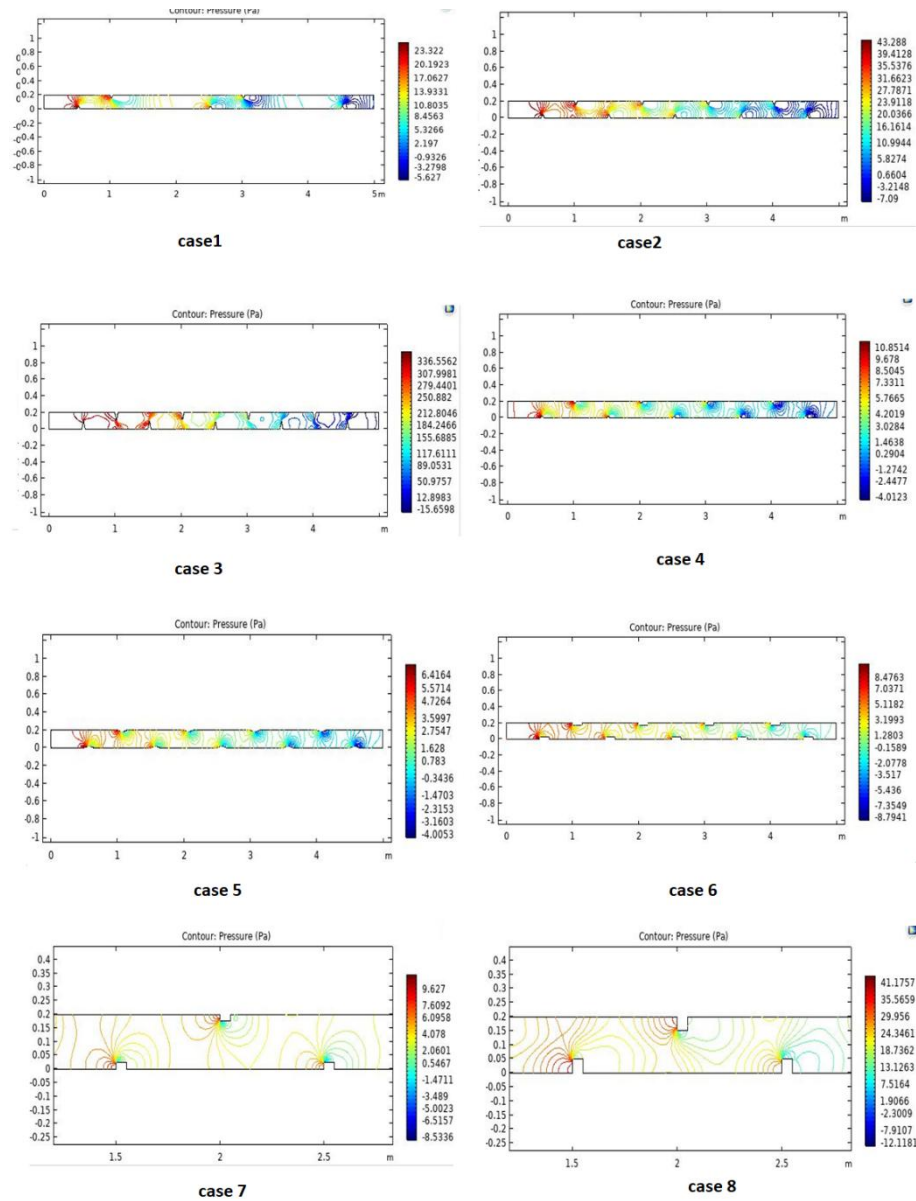


Fig. 6. The pressure Distribution contours.

### 4.3 | Pressure Distribution

Fig. 6 illustrates the pressure contours, showing that ribs not only create vortices but also induce pressure losses along the channel.

In case 1, the highest pressure occurs at the rib tip, while a negative pressure region develops near the channel outlet (Figs. 4 and 5).

In case 2, with 9 ribs, the pressure gradient reaches higher values in multiple locations, and backpressure increases (Figs. 4-8).

Adjusting the rib height and base length in Cases 3–5 intensifies local pressure gradients. Reducing the rib height lowers backpressure, as observed in case 4 (Fig. 4).

For rectangular ribs (Cases 6–8), pressure distribution varies with rib dimensions. Case 8 exhibits the highest backpressure and maximum local gradients (Fig. 4).

## 4.4 | Nusselt Number Distribution

The Nusselt number, representing convective heat transfer, is strongly affected by vortex formation. (Fig. 7)

In Case 1, the Nusselt number is nearly zero at the channel inlet, and increases after the flow interacts with the ribs.

In Case 2, stronger vortices due to a higher number of ribs lead to a significant increase in the Nusselt number.

In Cases 3 and 4, the rib height influences the turbulence intensity and Nusselt number. Case 4, with shorter ribs, shows lower Nusselt numbers than Case 2, indicating weaker turbulence.

For Cases 5–8, rectangular ribs affect the Nusselt number depending on rib geometry. Case 6 demonstrates the highest Nusselt values due to strong vortex formation (Fig. 4). Although Case 8 shows high velocity and pressure fluctuations, its Nusselt number is slightly lower than that of Case 6.

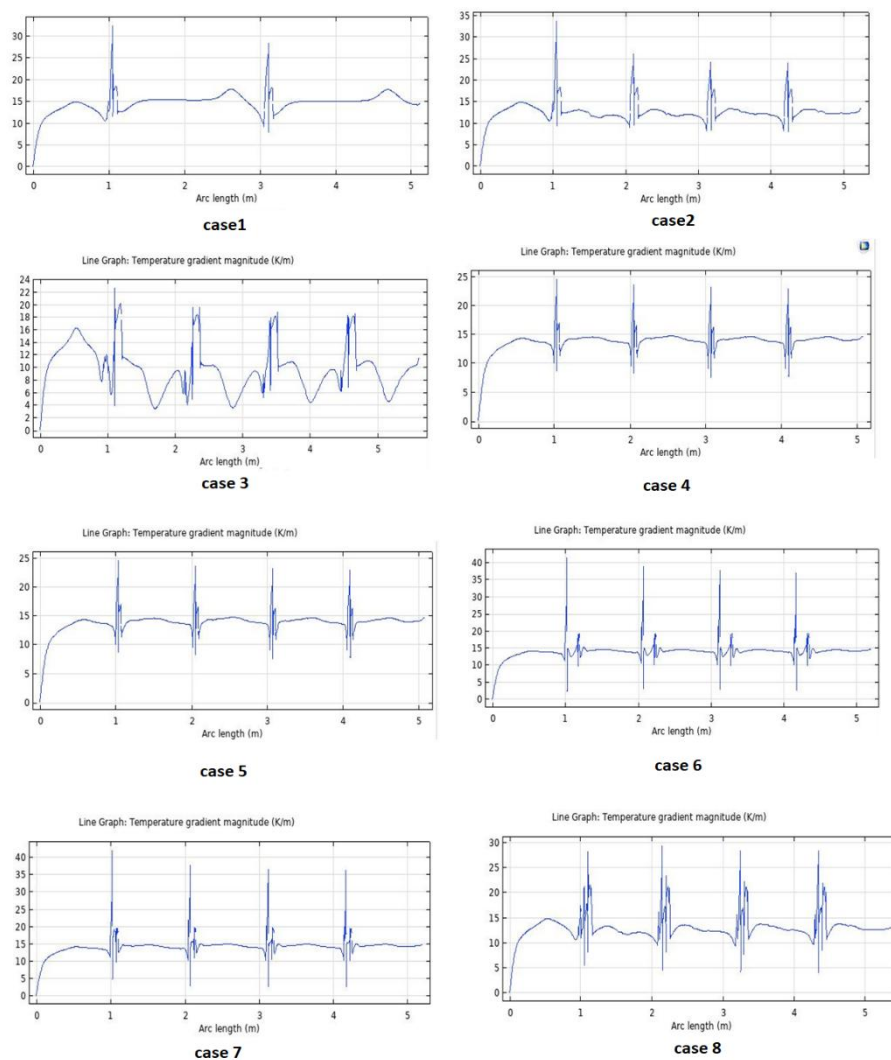


Fig. 7. Nusselt Number Distribution

## 5 | Conclusion

In this study, a detailed numerical analysis was performed to investigate the effects of discrete ribs on turbulent flow behavior and convective heat transfer in a rectangular channel. The influence of rib geometry,

number of ribs, rib height, and base length was systematically examined using a finite element framework coupled with the  $k-\omega$  SST turbulence model.

The results revealed that the presence of discrete ribs significantly alters the flow structure by inducing flow separation, recirculation regions, and secondary vortices, thereby effectively disrupting the thermal boundary layer and enhancing convective heat transfer. Increasing the number of ribs led to stronger turbulence generation and higher Nusselt numbers; however, this enhancement was accompanied by increased pressure losses along the channel. Rib height was found to strongly affect vortex intensity and heat transfer performance, with taller ribs intensifying flow disturbances but not always resulting in proportional HTE due to excessive pressure penalties.

Among the investigated geometries, rectangular ribs exhibited the highest heat transfer performance, owing to their ability to generate strong, sustained vortical structures downstream of each rib. In contrast, shorter ribs produced weaker flow disturbances but offered a more favorable balance between HTE and pressure drop. The distribution of the Nusselt number clearly correlated with vortex formation and reattachment zones, confirming the dominant role of flow dynamics in thermal enhancement mechanisms.

Overall, the present results highlight that an optimal rib configuration can significantly improve thermal performance while maintaining acceptable pressure losses. The findings of this study provide practical design guidelines for the development of advanced ribbed cooling channels in heat exchangers, turbine blade cooling systems, and electronic thermal management applications. Future work may extend the present analysis to three-dimensional configurations, transient flow conditions, and advanced working fluids such as nanofluids to further enhance thermal performance.

## Conflict of Interest

The authors declare no conflict of interest.

## Data Availability

All data are included in the text.

## Funding

This research received no specific grant from funding agencies in the public, commercial, or not-for-profit sectors.

## References

- [1] Liu, H., & Wang, J. (2011). Numerical investigation on synthetical performances of fluid flow and heat transfer of semiattached rib-channels. *International journal of heat and mass transfer*, 54(1–3), 575–583. <https://doi.org/10.1016/j.ijheatmasstransfer.2010.09.013>
- [2] Tanda, G. (2011). Effect of rib spacing on heat transfer and friction in a rectangular channel with 45 angled rib turbulators on one/two walls. *International journal of heat and mass transfer*, 54(5–6), 1081–1090. <https://doi.org/10.1016/j.ijheatmasstransfer.2010.11.015>
- [3] Chang, S. W., Liou, T. M., Chiang, K. F., & Hong, G. F. (2008). Heat transfer and pressure drop in rectangular channel with compound roughness of V-shaped ribs and deepened scales. *International journal of heat and mass transfer*, 51(3–4), 457–468. <https://doi.org/10.1016/j.ijheatmasstransfer.2007.05.010>
- [4] Yemenici, O., Firatoglu, Z. A., & Umur, H. I. (2012). An experimental investigation of flow and heat transfer characteristics over blocked surfaces in laminar and turbulent flows. *International journal of heat and mass transfer*, 55(13–14), 3641–3649. <https://doi.org/10.1016/j.ijheatmasstransfer.2012.02.064>
- [5] Yongsiri, K., Eiamsa-Ard, P., Wongcharee, K., & Eiamsa-Ard, S. (2014). Augmented heat transfer in a turbulent channel flow with inclined detached-ribs. *Case studies in thermal engineering*, 3, 1–10. <https://doi.org/10.1016/j.csite.2013.12.003>

- [6] Shen, Z., Xie, Y., & Zhang, D. (2015). Numerical predictions on fluid flow and heat transfer in U-shaped channel with the combination of ribs, dimples and protrusions under rotational effects. *International journal of heat and mass transfer*, 80, 494–512. <https://doi.org/10.1016/j.ijheatmasstransfer.2014.09.057>
- [7] Parsaiemehr, M., Pourfattah, F., Akbari, O. A., Toghraie, D., & Sheikhzadeh, G. (2018). Turbulent flow and heat transfer of Water/Al<sub>2</sub>O<sub>3</sub> nanofluid inside a rectangular ribbed channel. *Physica e: low-dimensional systems and nanostructures*, 96, 73–84. <https://doi.org/10.1016/j.physe.2017.10.012>
- [8] Wang, J., Liu, J., Wang, L., Sundén, B., & Wang, S. (2018). Numerical investigation of heat transfer and fluid flow in a rotating rectangular channel with variously-shaped discrete ribs. *Applied thermal engineering*, 129, 1369–1381. <https://doi.org/10.1016/j.applthermaleng.2017.09.142>
- [9] Srinivasan, S., Ekkad, S. V., & Tolpadi, A. (2018). Heat transfer measurements inside narrow channels with ribs and trenches. *Heat transfer engineering*, 39(9), 750–759. <https://doi.org/10.1080/01457632.2017.1341198>
- [10] Liu, J., Hussain, S., Wang, W., Xie, G., & Sundén, B. (2021). Experimental and numerical investigations of heat transfer and fluid flow in a rectangular channel with perforated ribs. *International communications in heat and mass transfer*, 121, 105083. <https://doi.org/10.1016/j.icheatmasstransfer.2020.105083>
- [11] Sivakumar, K., Kumar, T. S., Sivasankar, S., Ranjithkumar, V., & Ponshanmugakumar, A. (2021). Effect of rib arrangements on the flow pattern and heat transfer in internally ribbed rectangular divergent channels. *Materials today: proceedings*, 46, 3379–3385. <https://doi.org/10.1016/j.matpr.2020.11.548>
- [12] Bejan, A., & Kraus, A. D. (2003). *Heat transfer handbook* (Vol. 1). John Wiley & Sons. [https://www.academia.edu/download/37985766/Heat\\_Transfer\\_Handbook.pdf](https://www.academia.edu/download/37985766/Heat_Transfer_Handbook.pdf)
- [13] Lienhard, J. H. (2005). *A heat transfer textbook*. Phlogistron. [https://wiki.epfl.ch/me341-hmt/documents/Lienhard-Lienhard\\_2008\\_A%20heat%20transfer%20textbook%20ed3.pdf](https://wiki.epfl.ch/me341-hmt/documents/Lienhard-Lienhard_2008_A%20heat%20transfer%20textbook%20ed3.pdf)